

PAPER

Pilot-Aided Threshold Detection Combining for OFDM-CDMA Down Link Transmissions in a Frequency Selective Fading Channel

Tomoki SAO[†], *Student Member and* Fumiyuki ADACHI[†], *Regular Member*

SUMMARY In OFDM-CDMA down link (base-to-mobile) transmissions, each user's transmit data symbol is spread over a number of orthogonal sub-carriers using an orthogonal spreading sequence defined in the frequency-domain. The radio propagation channel is characterized by a frequency- and time-selective multipath fading channel (which is called a doubly selective multipath fading channel in this paper). Frequency-domain equalization is necessary at the receiver to restore orthogonality among different users. This requires accurate estimation of the time varying transfer function of the multipath channel. Furthermore, the noise enhancement due to orthogonality restoration degrades transmission performance. In this paper, pilot-aided threshold detection combining (TDC) is presented that can effectively suppress the noise enhancement. If the estimated channel gain is smaller than the detection threshold, it is replaced with the detection threshold in the frequency equalization. There exists an optimal threshold that can minimize the bit error rate (BER) for a given received E_b/N_0 . The average BER performance of OFDM-CDMA down link transmissions using the TDC is evaluated by computer simulations. It is found that TDC using optimum detection threshold can significantly reduce the BER floor and outperforms DS-CDMA with ideal rake combining.

key words: OFDM, CDMA, frequency-domain equalization, doubly selective multipath fading channel

1. Introduction

For future broadband wireless communications systems, some enhanced wireless techniques need to be developed for achieving very high-speed data transmissions or significantly increasing down link (base-to-mobile) capacity under severe fading environments [1]. Multi-carrier (MC) approach is a promising technique for high-speed data transmissions [2]–[7]. Increased down link capacity or higher-speed transmission capability may be achieved by the combination of MC and code division multiple access (CDMA) method [7]–[10]. Thus, recently, MC-CDMA has been attracting much attention for down link applications and is under extensive study. In MC-CDMA, each user's transmitting data symbol is spread over a number of different sub-carriers using an orthogonal spreading sequence defined in the frequency-domain. The MC-CDMA using orthogonal sub-carriers is called orthogonal frequency

division multiplexing (OFDM)-CDMA. In this paper, we consider the down link of an OFDM-CDMA mobile radio system (hereafter, which is called the OFDM-CDMA down link transmission system).

In mobile radio communications, the transmitted signal is reflected and diffracted by many obstacles between a transmitter and a receiver, thereby creating a multipath channel whose transfer function is not anymore constant over a signal bandwidth. Such a propagation channel is called a frequency-selective fading channel [11]. The received signal suffers from frequency distortion and thus, orthogonality destruction is produced, thereby producing large multi-user interference. A number of sophisticated multi-user interference suppression techniques have been proposed [8]–[10]. For the down link applications, the simplest multi-user interference suppression technique may be orthogonal restoring combining (ORC) that can perfectly eliminate the multi-user interference since all users' signals suffer from the same fading [9], [10]. In the ORC frequency equalization, accurate estimation of the time varying transfer function of the propagation channel is necessary. Furthermore, the noise enhancement due to orthogonality restoration degrades transmission performance because faded sub-carrier components tend to be multiplied by high gains in the frequency equalization process. To suppress the excessive noise enhancement, controlled equalization combining (CEC) was suggested in [9], in which the sub-carriers experiencing smaller channel gains than a detection threshold are removed from frequency equalization.

In this paper, a simple modification is made to the CEC for the reception of OFDM-CDMA signals so that the noise enhancement can be more effectively suppressed while minimizing the signal power loss. If the estimate of channel gain becomes too small such that a large noise enhancement may occur, it is replaced by a detection threshold in frequency equalization unlike from CEC. We call this equalization as threshold detection combining (TDC) in this paper. Similarly to CEC [9], there exists a trade-off relation between reducing the noise enhancement and increasing the multi-user interference due to partial orthogonality destruction. Computer simulations suggest [12] that with the optimum detection threshold, TDC can significantly im-

Manuscript received January 4, 2002.

Manuscript revised June 26, 2002.

[†]The authors are with the Electrical and Communication Engineering, Graduate School of Engineering, Tohoku University, Sendai-shi, 980-8579 Japan.

prove the average bit error rate (BER) performance compared to the ORC. Furthermore, the achievable average BER performance is superior to the direct sequence (DS)-CDMA using ideal rake reception. It will be shown that while the pilot-aided TDC is simple to implement, it can significantly reduce the BER floor compared to the ORC frequency equalization if the detection threshold is optimized.

The remainder of this paper is organized as follows. The OFDM-CDMA down link transmission system model is presented in Sect. 2. A single cell mobile communication system, i.e., one base station to communicate with all mobile users, is assumed. Section 3 presents the pilot-aided TDC. The computer simulation results are presented in Sect. 4 and the results are compared to DS-CDMA with ideal channel estimation. Section 5 concludes the paper.

2. OFDM-CDMA Down Link Transmission System

The transmitter and receiver model of the OFDM-CDMA down link transmission system is illustrated in Fig. 1.

2.1 Transmitter

The transmitter model is illustrated in Fig. 1(a). N

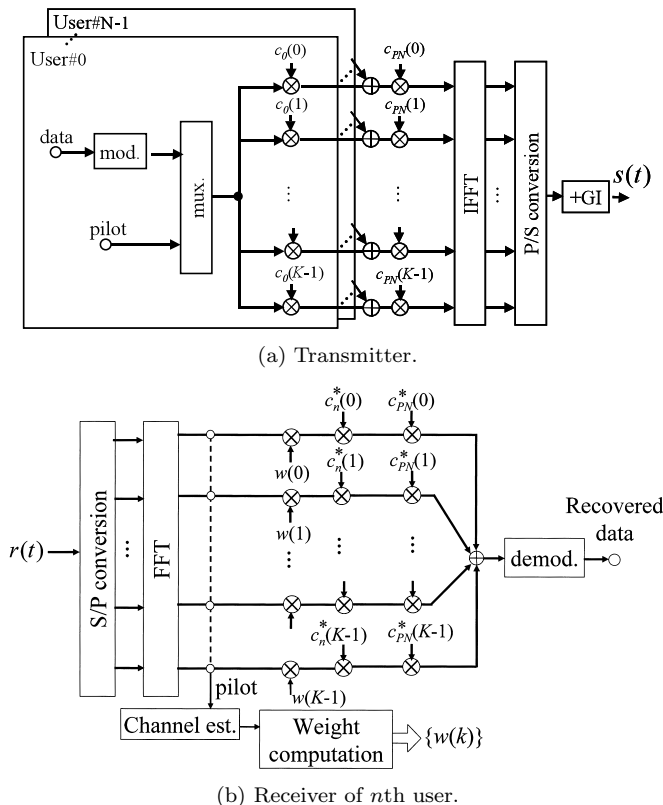


Fig. 1 Transmitter and receiver model for transmitting $m = 0$ th data symbol of $q = 0$ th slot.

users are assumed to be in communication. K orthogonal sub-carriers are used with frequency separation of $1/T_s$, where T_s denotes the effective symbol length of OFDM. At a base station, a binary transmission data is transformed into quaternary phase shift keying (QPSK)-modulated symbol sequence. We assume that the transmitted sequence has a slot structure which will be shown in Sect. 3. One slot consists of N_{slot} QPSK-symbols. The m th data symbol $d_n(qN_{slot} + m)$ of the q th slot of the n th user, $n = 0, 1, \dots, N$, is spread over K orthogonal sub-carriers using a K -length orthogonal spreading sequence $c_n(k) = \{-1, 1\}$ and then, multiplied by a long pseudo noise (PN) sequence $c_{PN}(i) = \{-1, 1\}$ with $i = (qN_{slot} + m)K + k$ for $k = 0, 1, \dots, K - 1$. Hence, the spreading factor (SF) is $SF = K$ for this transmission model. In Fig. 1, we assume to transmit the $m = 0$ th data symbol of the $q = 0$ th slot for simplicity. In this paper, we assume the single cell system. The PN sequence is used to randomize the multi-user interference produced by partial destruction of orthogonality due to imperfect frequency equalization. In the case of cellular systems, it is also used to randomize the multi-user interference produced by other users in other cells [13]. The sum of K data-modulated and coded sub-carrier components forms the OFDM-CDMA waveform of length T_s . This process can be performed using the inverse fast frequency transform (IFFT) [3]. Finally, a small portion of the OFDM-CDMA waveform is copied and added to it as a guard interval (GI), T_g , to form a resultant OFDM-CDMA symbol waveform of length $T = T_s + T_g$. If the time delay spread of the multipath channel is less than the guard interval, the orthogonality among sub-carriers can be maintained.

With N users' transmitting symbols being multiplexed, the composite symbol $u(k, qN_{slot} + m)$ of the q th slot for the k th sub-carrier can be expressed as

$$u(k, qN_{slot} + m) = \begin{cases} c_{PN}((qN_{slot} + m)K + k)p(k, qN_{slot} + m) & \text{for } 0 \leq m \leq N_p - 1 \\ c_{PN}((qN_{slot} + m)K + k) & \\ \cdot \sum_{n=0}^{N-1} c_n(k)d_n(qN_{slot} + m) & \\ \text{for } N_p \leq m \leq N_{slot} - 1 \end{cases} \quad (1)$$

with $0 \leq k \leq K - 1$, where $p(k, qN_{slot} + m)$ represents the pilot symbol which is shared by all users (see Sect. 3.1) and $|d_n(k)| = 1$. The orthogonal spreading sequence $\{c_n(k)\}$ has a length of K and satisfies

$$\sum_{k=0}^{K-1} c_n(k)c_i^*(k) = \begin{cases} K & \text{for } n = i \\ 0 & \text{for } n \neq i \end{cases}, \quad (2)$$

where $(\cdot)^*$ denotes complex conjugate (although binary sequences are assumed in this paper, the complex notation is used here). The length of PN sequence $\{c_{PN}(i)\}$

is much longer than K .

The OFDM-CDMA signal waveform is expressed in the equivalent baseband representation as

$$s(t) = \sum_{q=-\infty}^{\infty} \sum_{m=0}^{N_{slot}-1} g(t - (qT_{slot} + mT)) \cdot \left\{ \sqrt{\frac{2S}{K}} \sum_{k=0}^{K-1} u(k, qN_{slot} + m) \cdot \exp[j2\pi(t - (qT_{slot} + mT))k/T_s] \right\}, \quad (3)$$

where S denotes the average signal power per user, T denotes the OFDM-CDMA symbol length which was already introduced and is given by

$$T = T_g + T_s, \quad (4)$$

$g(t)$ denotes the transmit pulse given by

$$g(t) = \begin{cases} 1, & \text{for } -T_g \leq t \leq T_s \\ 0, & \text{otherwise} \end{cases}, \quad (5)$$

and $T_{slot} = N_{slot}T$ is the slot length in time.

2.2 Radio Propagation Channel

The OFDM-CDMA down link signal is transmitted from the base station to a mobile station. Assuming the radio propagation channel has L discrete paths having different time delays, the channel impulse response $h(\tau, t)$ at time t is represented as

$$h(\tau, t) = \sum_{l=0}^{L-1} \xi_l(t) \delta(\tau - \tau_l), \quad (6)$$

where $\xi_l(t)$ and τ_l are respectively the complex channel gain and time delay of the l th path with $\sum_{l=0}^{L-1} E[|\xi_l(t)|^2] = 1$, where $E[\cdot]$ denotes the ensemble average. It is assumed that $h(\tau, t)$ exists only in an interval of $0 \leq \tau \leq T_g$, i.e., $\{\tau_l\}_{\max} \leq T_g$. The channel transfer function $H(f, t)$ becomes

$$\begin{aligned} H(f, t) &= \int_0^{\infty} h(\tau, t) \exp(-j2\pi f\tau) d\tau \\ &= \sum_{l=0}^{L-1} \xi_l(t) \exp(-j2\pi f\tau_l). \end{aligned} \quad (7)$$

When multiple paths exist ($L > 1$), the resultant transfer function becomes a complex function of frequency. Such a channel is called the frequency-selective fading channel. Furthermore, the shape of the transfer function varies in time in a random manner according to the user's movement, resulting in a doubly selective multipath fading channel.

2.3 Receiver

Figure 1(b) illustrates the n th user's mobile receiver

structure. The frequency-distorted received signal is decomposed into K sub-carrier components (this is done by FFT) and then, frequency-equalized to restore the orthogonality among different users. Frequency equalization requires estimation of the propagation channel transfer function (this is called channel estimation). The frequency-equalized n th user's K sub-carrier components are first multiplied by the long PN sequence $\{c_{PN}(i); i = (qN_{slot} + m)K, (qN_{slot} + m)K + 1, \dots, (qN_{slot} + m + 1)K - 1\}$, then, multiplied by the orthogonal spreading sequence $\{c_n(k); k = 0, 1, \dots, K - 1\}$ and summed up.

The received signal is the convolution of the transmitted signal and the channel impulse response and its equivalent baseband representation is expressed as

$$r(t) = \int_{-\infty}^{\infty} h(\tau, t) s(t - \tau) d\tau + n(t), \quad (8)$$

where $n(t)$ denotes the additive white Gaussian noise (AWGN) with the single-sided power spectrum density N_0 . The equivalent baseband representation of the k th sub-carrier component $\tilde{r}(k, qN_{slot} + m)$ of the received OFDM-CDMA down link signal is given by

$$\begin{aligned} \tilde{r}(k, qN_{slot} + m) &= \frac{1}{T_s} \int_{qT_{slot} + mT}^{qT_{slot} + mT + T_s} r(t) \exp[-j2\pi(t - (qT_{slot} + mT))k/T_s] dt \\ &= \sqrt{\frac{2S}{K}} \sum_{i=0}^{K-1} u(i, qN_{slot} + m) \cdot \frac{1}{T_s} \int_0^{T_s} \exp[j2\pi(i - k)t/T_s] \\ &\quad \cdot \left\{ \int_{-\infty}^{\infty} h(\tau, t + qT_{slot} + mT) g(t - \tau) \cdot \exp(-j2\pi i\tau/T_s) d\tau \right\} dt + \tilde{n}(k, qN_{slot} + m), \end{aligned} \quad (9)$$

where $\tilde{n}(k, qN_{slot} + m)$ is the complex-valued Gaussian noise with variance $2N_0/T_s$ owing to the AWGN. Since we are assuming that $h(\tau, t)$ exists only in the interval $0 \leq \tau \leq T_g$ and from Eq. (5), we have

$$\begin{aligned} &\int_{-\infty}^{\infty} h(\tau, t + qT_{slot} + mT) g(t - \tau) \exp(-j2\pi i\tau/T_s) d\tau \\ &= \int_0^{T_g} h(\tau, t + qT_{slot} + mT) \exp(-j2\pi i\tau/T_s) d\tau \\ &= H(i/T_s, t + qT_{slot} + mT). \end{aligned} \quad (10)$$

It is assumed that $\xi_l(t)$ varies very slowly and stays constant over an interval of T , i.e.,

$$\xi_l(t + qT_{slot} + mT) \approx \xi_l(qT_{slot} + mT)$$

$$\text{for } 0 \leq t < T. \quad (11)$$

Since

$$\begin{aligned} H(i/T_s, t + qT_{slot} + mT) &\approx H(i/T_s, qT_{slot} + mT) \\ \text{for } 0 \leq t < T, \end{aligned} \quad (12)$$

Equation (9) can be rewritten as

$$\begin{aligned} &\tilde{r}(k, qN_{slot} + m) \\ &\approx \frac{1}{T_s} \sqrt{\frac{2S}{K}} \sum_{i=0}^{K-1} u(i, qN_{slot} + m) \\ &\quad \cdot H(i/T_s, qT_{slot} + mT) \\ &\quad \cdot \int_0^{T_s} \exp[j2\pi(i-k)t/T_s] dt + \tilde{n}(k, qN_{slot} + m) \\ &= \sqrt{\frac{2S}{K}} H(k/T_s, qT_{slot} + mT) u(k, qN_{slot} + m) \\ &\quad + \tilde{n}(k, qN_{slot} + m). \end{aligned} \quad (13)$$

It is understood from Eq. (13) that the frequency equalization is necessary to restore the orthogonality among different users. Thus, estimation of the channel transfer function $H(k/T_s, qT_{slot} + mT)$ is necessary (channel estimation) to compute the frequency equalization weight $w(k/T_s, qN_{slot} + m)$. After equalization, K sub-carrier components $\{\tilde{r}(k, qN_{slot} + m); k = 0, 1, \dots, K-1\}$ are multiplied by the long PN sequence $\{c_{PN}((qN_{slot} + m)K + k); k = 0, 1, \dots, K-1\}$ and then the orthogonal spreading sequence $\{c_n(k)\}$ to be summed up. As a consequence, the n th user's m th data symbol $\hat{d}_n(qN_{slot} + m)$ in the q th slot is obtained as

$$\begin{aligned} &\hat{d}_n(qN_{slot} + m) \\ &= \sum_{k=0}^{K-1} w(k, qN_{slot} + m) \tilde{r}(k, qN_{slot} + m) \\ &\quad \cdot c_n^*(k) c_{PN}^*((qN_{slot} + m)K + k), \end{aligned} \quad (14)$$

which is the decision variable to decide as to which symbol was transmitted.

The frequency equalization weight for ORC is given by Eq.(18). If ideal channel estimation is assumed, i.e., $\hat{H}(k/T_s, qT_{slot} + mT) = H(k/T_s, qT_{slot} + mT)$ in Eq.(18), the n th user's received symbol $\hat{d}_n(qN_{slot} + m)$ is from Eq. (14)

$$\begin{aligned} &\hat{d}_n(qN_{slot} + m) \\ &= \sqrt{2SK} d_n(qN_{slot} + m) \\ &\quad + \sum_{k=0}^{K-1} \frac{\tilde{n}(k, qN_{slot} + m)}{H(k/T_s, qT_{slot} + mT)} \\ &\quad \cdot c_n^*(k) c_{PN}^*((qN_{slot} + m)K + k). \end{aligned} \quad (15)$$

It is understood that no multi-user interference is produced, however, the noise power is enhanced at sub-carriers where the channel gain becomes weak.

In this paper, we apply a pilot-aided channel estimation to estimate $H(k/T_s, qT_{slot} + mT)$ and threshold detection is introduced into frequency equalization.

However, since channel estimation error exists, both noise enhancement and multi-user interference due to partial orthogonality destruction are produced, thereby seriously degrading the BER performance. This will be discussed in the next section.

3. Pilot-Aided TDC

3.1 Pilot-Aided Channel Estimation

As used in channel estimation for coherent rake combining of DS-CDMA signal [14], the known pilot symbols are time-multiplexed onto the transmitting data symbol sequence for channel estimation at a receiver. Here, we assume that N_p pilot symbols are time-multiplexed every N_d data symbols, where N_p pilot symbols and succeeding N_d data symbols forms a slot with symbol length of $N_{slot} = N_p + N_d$. For down link (base-to-mobile) transmission system, pilot symbols can be shared by all users. Figure 2 illustrates the frequency-time space representation of the slot structure. Each pilot symbol is transmitted on all sub-carriers. Figure 3 shows the power distribution in a slot (for simplicity, only two users are assumed), where the pilot power is

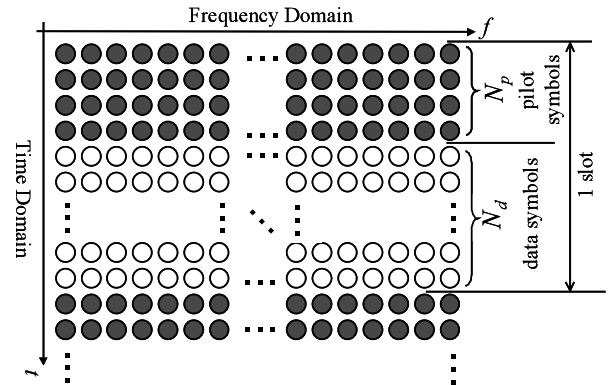


Fig. 2 Slot structure.

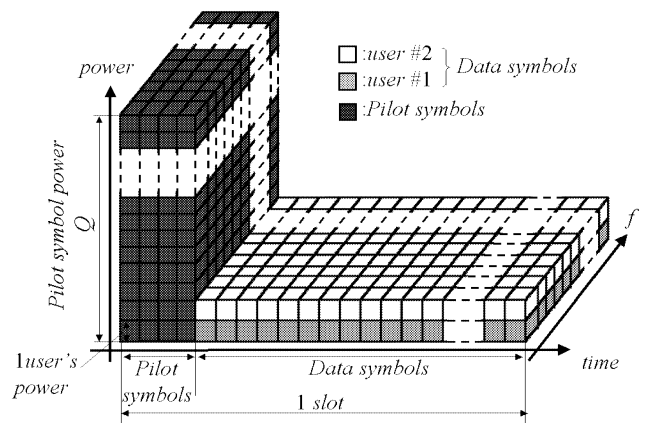


Fig. 3 Power distribution (for simplicity purpose, two-user case is shown).

Q times larger than data symbol where Q is ratio of the pilot symbol-to-data symbol power per user.

First, we estimate the instantaneous channel gain at the beginning of each slot by summing up N_p pilot symbols. The instantaneous channel estimate $\tilde{H}(k/T_s, qT_{slot})$ at the k th sub-carrier frequency position is given by

$$\begin{aligned} \tilde{H}(k/T_s, qT_{slot}) &= \frac{1}{N_p \sqrt{2SQ/K}} \sum_{m=0}^{N_p-1} \tilde{r}(k, qN_{slot} + m) \\ &\quad \cdot p^*(k, qN_{slot} + m) \cdot c_{PN}^*((qN_{slot} + m)K + k), \end{aligned} \quad (16)$$

where $\{p(k, qN_{slot} + m); 0 \leq m \leq N_p - 1\}$ are the transmitted pilot symbols. (Note that the denominator can be removed from Eq. (16) since it is the same for all sub-carrier components.) Without loss of generality, we assume

$$p(k, qN_{slot} + m) = \sqrt{Q} \exp(j\pi/4). \quad (17)$$

The channel estimate to be used for frequency equalization is $\tilde{H}(k/T_s, qT_{slot} + mT) = \tilde{H}(k/T_s, qT_{slot})$ for $N_p \leq m \leq N_{slot} - 1$.

3.2 ORC

For frequency equalization of N_d data symbols of the q th slot,

$$\begin{aligned} w_{ORC}(k, qN_{slot} + m) &= \frac{\tilde{H}^*(k/T_s, qT_{slot} + mT)}{|\tilde{H}(k/T_s, qT_{slot} + mT)|^2} \end{aligned} \quad (18)$$

is used in Eq. (14) and we have

$$\begin{aligned} \hat{u}(k, qN_{slot} + m) &= w_{ORC}(k, qN_{slot} + m) \tilde{r}(k, qN_{slot} + m) \\ &= \sqrt{\frac{2S}{K}} \alpha(k, qN_{slot} + m) u(k, qN_{slot} + m) \\ &\quad + \frac{\tilde{n}(k, qN_{slot} + m)}{\tilde{H}(k/T_s, qT_{slot} + mT)}, \end{aligned} \quad (19)$$

where

$$\alpha(k, qN_{slot} + m) = \frac{H(k/T_s, qT_{slot} + mT)}{\tilde{H}(k/T_s, qT_{slot} + mT)}. \quad (20)$$

As described in Sect.3.1, the decision variable $\hat{d}_n(qN_{slot} + m)$ for the n th user's m th data symbol in the q th slot is obtained as

$$\hat{d}_n(qN_{slot} + m) = \sum_{k=0}^{K-1} \hat{u}(k, qN_{slot} + m) c_{PN}^*((qN_{slot} + m)K + k) c_n^*(k)$$

$$\begin{aligned} &= \sqrt{\frac{2S}{K}} d_n(qN_{slot} + m) \left(\sum_{k=0}^{K-1} \alpha(k, qN_{slot} + m) \right) \\ &\quad + \sqrt{\frac{2S}{K}} \sum_{\substack{i=0 \\ i \neq n}}^{K-1} d_i(qN_{slot} + m) \\ &\quad \cdot \sum_{k=0}^{K-1} \alpha(k, qN_{slot} + m) c_i(k) c_n^*(k) \\ &\quad + \sum_{k=0}^{K-1} \frac{\tilde{n}(k, qN_{slot} + m)}{\tilde{H}(k/T_s, qT_{slot} + mT)} \\ &\quad \cdot c_{PN}^*((qN_{slot} + m)K + k) c_n^*(k). \end{aligned} \quad (21)$$

The first term of Eq. (21) is the desired component, the second term the multi-user interference, and the third the noise component.

3.3 CEC

To suppress the noise enhancement produced in the ORC, the CEC was proposed, in which the subcarrier components of weaker channel gains than the predetermined threshold h_{th} are removed from combining [9]. The combining weight $w_{CEC}(k, qN_{slot} + m)$ is given by

$$\begin{aligned} w_{CEC}(k, qN_{slot} + m) &= \begin{cases} \frac{1}{\tilde{H}(k/T_s, qT_{slot} + mT)}, \\ \text{if } |\tilde{H}(k/T_s, qT_{slot} + mT)| \geq h_{th} \\ 0, \text{ otherwise.} \end{cases} \end{aligned} \quad (22)$$

As the value of h_{th} becomes larger, the noise enhancement can be suppressed, but the multi-user interference (MUI) increases due to larger orthogonality destruction. Therefore, there exists the optimum value in h_{th} .

3.4 TDC

To avoid a large noise enhancement, limiting the value of weight less than a certain maximum value is introduced [12]. For frequency equalization in Eq. (14), we use

$$\begin{aligned} w_{TD}(k, qN_{slot} + m) &= \begin{cases} \frac{\tilde{H}^*(k/T_s, qT_{slot} + mT)}{|\tilde{H}(k/T_s, qT_{slot} + mT)|^2}, \\ \text{if } |\tilde{H}(k/T_s, qT_{slot} + mT)| \geq h_{th} \\ \frac{1}{h_{th}} \frac{|\tilde{H}(k/T_s, qT_{slot} + mT)|}{\tilde{H}(k/T_s, qT_{slot} + mT)}, \\ \text{otherwise} \end{cases} \end{aligned} \quad (23)$$

where h_{th} is the detection threshold. Similarly to the CEC, there exists the optimum value in h_{th} .

4. Computer Simulation

4.1 Simulation Condition

Computer simulation condition is summarized in Table 1. The sampling period Δ for IFFT and FFT is $\Delta = T_s/K$ and equals T_s/SF in this paper. To make the transmission bandwidths of OFDM-CDMA and DS-CDMA equal, Δ is set to $\Delta = T_c$, where T_c represents the DS-CDMA chip length. The spreading factor (SF) is SF=256 for both OFDM-CDMA and DS-CDMA and the maximum number of users to be accommodated is 256. The symbol rate of OFDM-CDMA is 8/9 times that of DS-CDMA since the transmission bandwidth equals $1/T_c = 256/T_s$ in both OFDM-CDMA and DS-CDMA systems. The propagation channel is assumed to have $L = 2$ paths, each path experiencing independent Rayleigh fading with equal variance (uniform power delay profile), i.e., $E[|\xi_0|^2] = E[|\xi_1|^2] = 1/2$, and delay difference of $\tau_1 - \tau_0 = 5T_c$. In the following computer simulation, the pilot power-to-data symbol power per user ratio is assumed to be $Q = 256$ (see Fig. 3). Throughout the following computer simulations, we set the number of pilot symbols $N_p = 4$ and that of data symbols $N_d = 60$ per slot (hence, $N_{slot} = 64$). For performance comparison, DS-CDMA transmission is also considered. $L = 2$ -finger rake reception with ideal channel estimation [15] is assumed.

4.2 Finding the Optimum Detection Threshold

Since the propagation channel is doubly selective, the channel transfer function may vary over the time interval of one slot according to the user's movement. In addition, as the channel gains are time varying, the frequency locations experiencing deep fades in the channel transfer function are also time varying. This is seen in Fig. 4, which plots the channel transfer functions at the beginning and the end of the slot. However, since channel estimation is performed only at the beginning of each slot, larger equalization error occurs in a fast fading channel when equalizing the received data symbols closer to the end of the slots, thereby producing BER

Table 1 Simulation condition (down link transmission).

Data modulation		QPSK
Spreading codes	Orthogonal code	SF=256
	Scramble code	PN with 4095 chips
OFDM-CDMA	No. of subcarriers	$K=256$
	Effective symbol length	$T_s=256T_c$
	Guard interval	$T_g=32T_c$ ($T_g/T_s=1/8$)
Rayleigh fading channel	No. of paths	$L=2$
	Time delay	$\tau=5T_c$

floor. By changing the threshold value in TDC, the BER floor can be controlled.

Figure 5 plots the BER performance as a function of the average received signal energy per information bit-to-AWGN power spectrum density ratio E_b/N_0 with the detection threshold h_{th} as a parameter for the case of $N = 128$ users and the normalized fading maximum Doppler frequency of $f_D T_{slot} = 0.0064$ (i.e., $f_D T = 0.0001$). In the low E_b/N_0 region, where the AWGN is a major cause of decision errors, the BER performance improves due to suppression of noise enhancement and a better BER performance is achieved compared to that of no detection threshold, i.e., ORC frequency equalization. However, BER floors are observed in the high E_b/N_0 region. The BER floor starts to decrease as the detection threshold becomes larger, but increases when the detection threshold value ex-

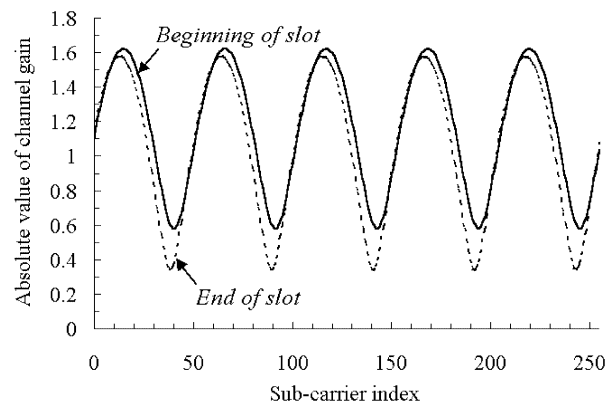


Fig. 4 Instantaneous transfer functions measured at the beginning and the end of the slot for $f_D T_{slot} = 0.064$.

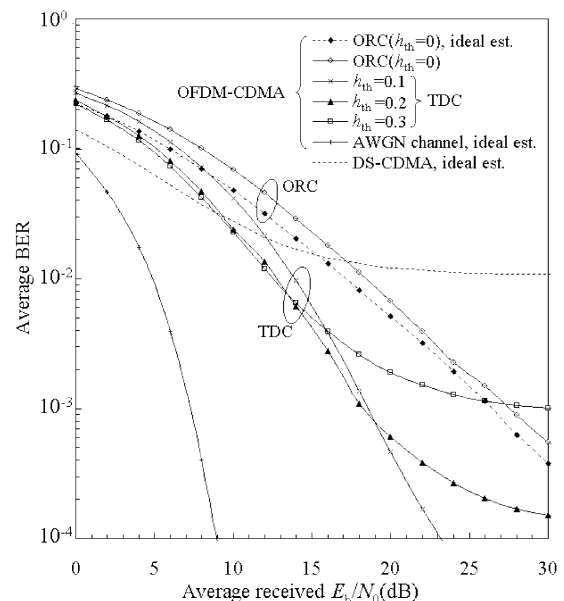


Fig. 5 Simulated BER performance for $N = 128$ and $f_D T_{slot} = 0.0064$.

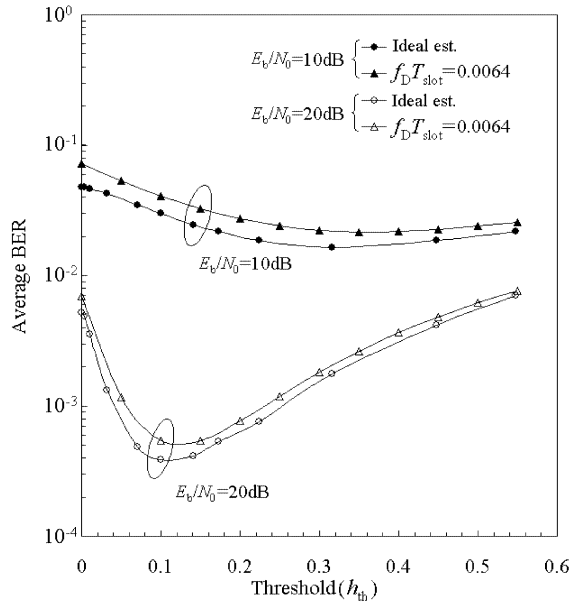


Fig. 6 Impact of detection threshold on achievable average BER at average $E_b/N_0=10$ dB and 20 dB for $f_D T_{slot} = 0.0064$ and $N = 128$.

ceeds a certain value.

As seen in Fig. 5, the optimum detection threshold that minimizes the average BER may be different for the different average E_b/N_0 value. Figure 6 plots the achievable average BER values at the average $E_b/N_0 = 10$ dB and 20 dB as a function of the detection threshold when $f_D T_{slot} = 0.0064$. A broader optimum region in the detection threshold is seen for the average $E_b/N_0 = 10$ dB compared to the average $E_b/N_0 = 20$ dB. Furthermore, the optimum detection threshold is almost the same as in the case of ideal channel estimation. The optimum detection threshold is around $h_{th} = 0.3$ and 0.1 for the average $E_b/N_0 = 10$ dB and 20 dB, respectively. The average BER performance with TDC using optimum detection threshold at each E_b/N_0 value is plotted in Fig. 7. The E_b/N_0 degradation with optimum detection threshold is found to be as small as 0.6 dB compared to ideal channel estimation for BER=0.001. Furthermore, the required E_b/N_0 can be reduced by about 9.5 dB compared to ORC (i.e., no detection threshold ($h_{th} = 0$)). It is clearly seen that although BER floors are seen, the BER performance is better than that of DS-CDMA using ideal rake combining.

4.3 Impact of Time Delay

When the time delay difference τ between the two paths is zero (or the propagation channel has a single path), no orthogonality destruction occurs and hence, no MUI is produced. As the time delay difference increases, the channel becomes frequency selective and the orthogonality property among users starts to be destroyed,

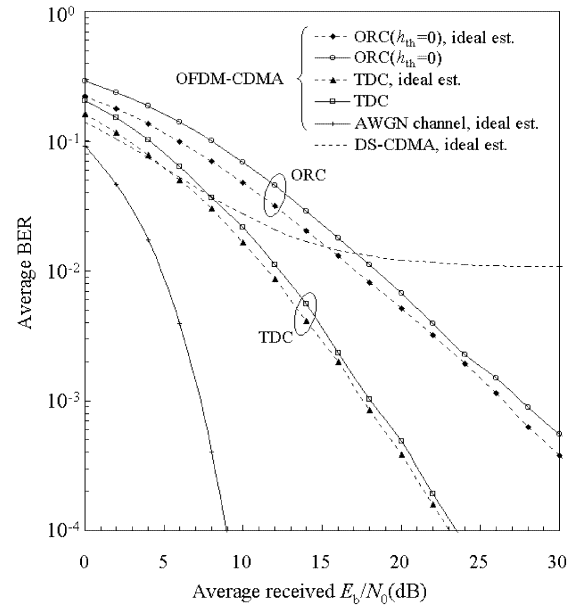


Fig. 7 Simulated BER performance with frequency equalization using optimum detection threshold for $f_D T_{slot} = 0.0064$ and $N = 128$.

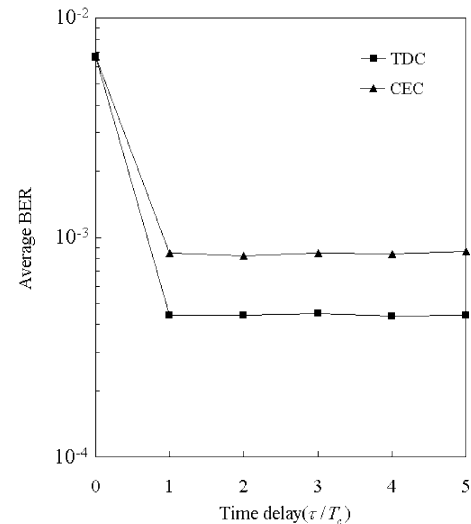


Fig. 8 Effect of time delay difference between two paths on achievable BER for $N = 128$, the average received $E_b/N_0 = 20$ dB, and $f_D T_{slot} = 0.0064$.

thereby producing MUI. The use of ORC produces the noise enhancement in exchange for the orthogonality restoration. This results in increased BER as seen in Fig. 8. For the time delay difference of $\tau \geq 1T_c$, the noise enhancement is produced in ORC, while TDC and CEC reduce the average BERs due to the frequency diversity effect. It can be seen from Fig. 8 that the frequency diversity effect remains constant for $\tau \geq 1T_c$.

4.4 Impact of Fading Rate

The dependence of the optimum detection threshold on

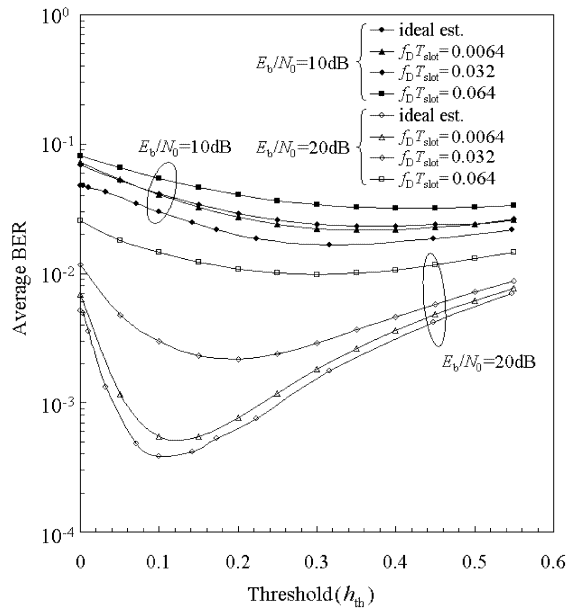


Fig. 9 Impact of $f_D T_{slot}$ on achievable average BER at average $E_b/N_0=10$ dB and 20 dB for $N = 128$.

the fading rate was evaluated. The achievable average BER values at the average $E_b/N_0=10$ dB and 20 dB are plotted as a function of the detection threshold in Fig. 8 for $f_D T_{slot} = 0.0064, 0.032$ and 0.064 (i.e., $f_D T = 0.0001, 0.0005$ and 0.001). In a fast fading channel, the transfer function varies during the reception of data symbols in a slot. However, the channel estimation is done only at the beginning of each slot. Hence, as the fading rate increases, the BER increases as discussed previously, but the optimum detection threshold is almost insensitive to the fading rate. This is clearly seen in Fig. 9. The BER performance with TDC using optimum detection threshold at each E_b/N_0 value is plotted in Fig. 10 for $f_D T_{slot} = 0.0064, 0.032$ and 0.064 . It is clearly seen that the BER floor increases as the fading rate becomes larger, but it is still smaller than that of DS-CDMA using ideal channel estimation.

4.5 Performance Comparison with CEC

Our computer simulation found that the optimum detection threshold of CEC is slightly smaller than that of TDC. This is shown in Fig. 11 that plots the average BERs at the average $E_b/N_0 = 10$ dB and 20 dB as a function of the detection threshold for $f_D T_{slot} = 0.032$ and $N = 128$. The optimum detection threshold of TDC is 0.2 (0.35) while that of CEC is 0.1 (0.2) for the average $E_b/N_0 = 10$ (20) dB. The results plotted in Fig. 11 are in the case of $L = 2$. The same computer simulations were conducted for $L = 3$ and 4. It was found that the optimum thresholds of TDC and CEC are almost insensitive to the value of L and that their BERs with optimum detection thresholds decrease for increasing L due to increasing frequency diversity ef-

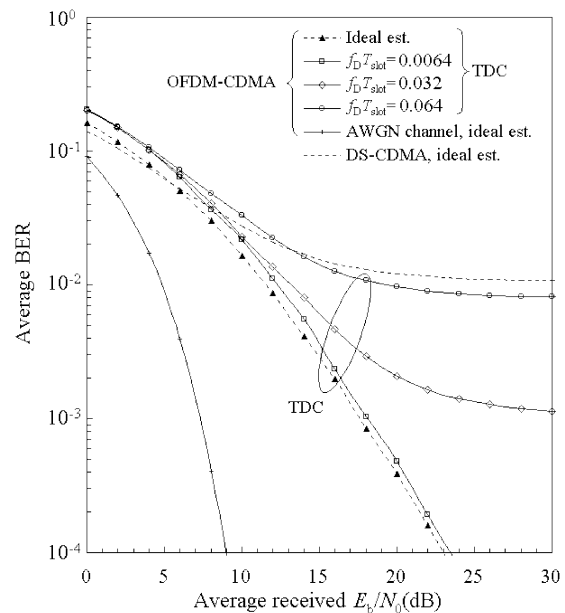


Fig. 10 Impact of $f_D T_{slot}$ on BER performance with TDC using optimum detection threshold for $N = 128$.

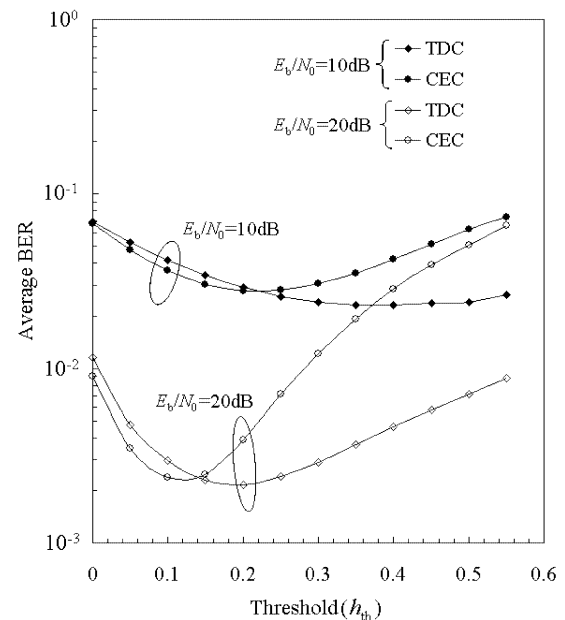


Fig. 11 Impact of detection threshold on achievable average BER at average $E_b/N_0=10$ dB and 20 dB for $f_D T_{slot} = 0.032$ and $N = 128$.

fect, but the TDC provides always better BER performance than CEC irrespective of value of L .

In Fig. 12, the BER performance with TDC is compared to that with CEC for $f_D T_{slot} = 0.032$. TDC provides better BER performance than CEC. In the low E_b/N_0 region, where the AWGN is a major cause of transmission errors, the BER performance using TDC is about 1 dB superior to that using CEC. The BER floor seen in high E_b/N_0 regions is smaller with TDC.

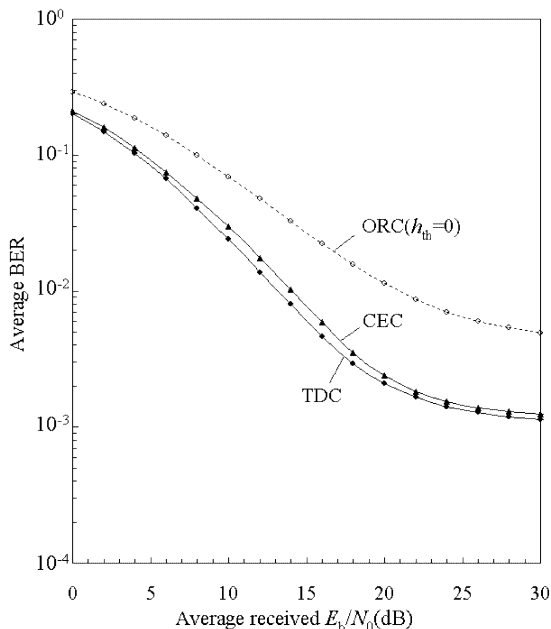


Fig. 12 Performance comparison of TDC and CEC. Optimum detection thresholds are used in both equalization schemes. $f_D T_{slot} = 0.032$. $N = 128$.

This is because, in CEC, the baseband components of sub-carriers experiencing smaller channel gains than the detection threshold are completely removed from frequency equalization, while all the sub-carrier components are utilized in TDC.

4.6 Performance Comparison with the Single User Case

Using threshold detection in the frequency equalization improves the BER performance by suppressing the noise enhancement at the cost of the orthogonal destruction. It is interesting to see how the achievable BER performance approaches that of the single user case.

In the single user case ($N = 1$), frequency equalization is not necessary. The best combining scheme is the maximal ratio combining (MRC) [11] in the frequency-domain. The frequency-domain MRC is performed as follows. We consider the $n = 0$ th user. The K sub-carrier components, $\{\tilde{u}(k, qN_{slot} + m); k = 0, 1, \dots, K - 1\}$, obtained by performing FFT, are first multiplied by $\tilde{H}^*(k/T_s, qN_{slot})$ instead of dividing by it. Then, they are multiplied by the orthogonal spreading sequence $\{c_0(k)\}$ and the long PN sequence $\{c_{PN}((qN_{slot} + m)K + k)\}$, and finally summed up to obtain the m th data symbol $\hat{d}_0(qN_{slot} + m)$ in the q th slot:

$$\begin{aligned} \hat{d}_0(qN_{slot} + m) &= \sum_{k=0}^{K-1} \tilde{u}(k, qN_{slot} + m) \tilde{H}^*(k/T_s, qT_{slot}) \end{aligned}$$

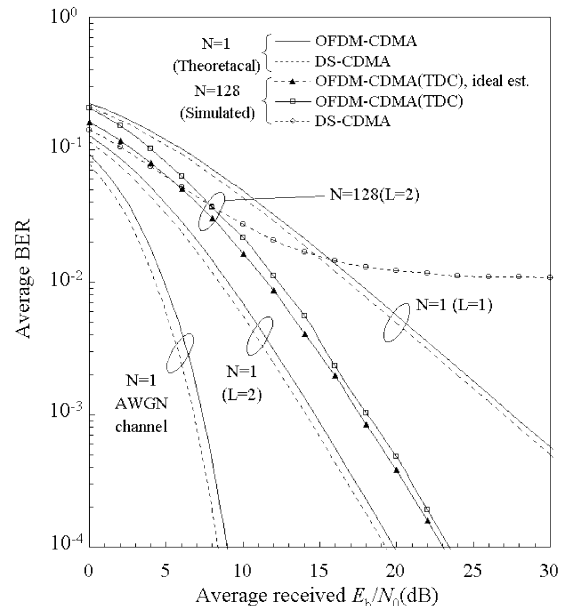


Fig. 13 Comparison of BER performances for $N = 128$ users case (simulated) and single user case (theoretical). $f_D T_{slot} = 0.0064$.

$$\cdot c_{PN}^*((qN_{slot} + m)K + k)c_0^*(k), \quad (24)$$

where $N_p \leq m \leq N_{slot} - 1$, which is the decision variable. The average BER performance of OFDM-CDMA with the above frequency-domain MRC for the single user case is theoretically derived in Appendix (also presented in Appendix is the theoretical average BER of DS-CDMA with ideal rake combining). Figure 13 plots the theoretical average BER performances of OFDM-CDMA with the frequency-domain MRC and DS-CDMA with ideal rake combining for the single user case and compared to the simulation results with TDC using optimum detection threshold for $N = 128$ users case. $T_g/T_s = 1/8$ is assumed as shown in the simulation condition. It is seen from Fig. 11 that the simulated BER performance of OFDM-CDMA with TDC for the $N = 128$ users case is better than the theoretical BER performance for single user case of $L = 1$ and is close to the theoretical BER performance for the single user case of $L = 2$. This shows that using TDC provides frequency diversity effect in a frequency selective fading channel. When $L = 2$, the performance degradation from the theoretical single user case is about 2.8 dB (ideal channel estimation) and about 3.6 dB (pilot-aided channel estimation).

5. Conclusion

In the OFDM-CDMA down link transmission system, frequency equalization is necessary to restore the orthogonality in a frequency selective fading channel. However, frequency equalization requires accurate estimation of channel transfer function and also produces the noise enhancement. In this paper, pilot-aided

threshold detection combining (TDC) was presented that can effectively suppress the noise enhancement. If the estimates of channel gain at some sub-carriers become too small such that a large noise enhancement may occur, they are replaced with the detection threshold unlike the controlled equalization combining (CEC) of [9] (i.e., instead of completely removing those sub-carrier components from frequency equalization).

The BER performance of OFDM-CDMA down link transmission using the pilot-aided TDC was evaluated by computer simulations. The optimum threshold exists in the detection threshold due to trade off relation between reducing the noise enhancement and increasing the orthogonality destruction. It depends on the average E_b/N_0 but is almost insensitive to the fading rate. When using the optimum detection threshold at each E_b/N_0 value, the TDC can achieve better BER performance compared to the ORC frequency equalization using ideal channel estimation. Although the BER floor is observed in a fast fading channel (no BER floor is produced with ORC frequency equalization using ideal channel estimation), the use of the optimum detection threshold in TDC can significantly reduce the BER floor. The BER performance with TDC was also compared to that with CEC. It was found that TDC can achieve better BER performance. This is because the baseband components of sub-carriers experiencing smaller channel gains than the detection threshold are completely removed from frequency equalization in CEC, while all the sub-carrier components are utilized in TDC. Furthermore, it was found that a better BER performance is achieved than DS-CDMA with ideal rake combining.

References

- [1] F. Adachi, "Wireless past and future—Evolving mobile communications systems," IEICE Trans. Fundamentals, vol.E83-A, no.1, pp.55–60, Jan. 2001.
- [2] V. Mignone and A. Morello, "CD3-OFDM: A novel demodulation scheme for fixed and mobile receivers," IEEE Trans. Commun., vol.44, no.9, pp.1144–1151, Sept. 1996.
- [3] S. Hara, M. Mouri, M. Okada, and N. Morinaga, "Transmission performance analysis of multicarrier modulation in frequency selective fast Rayleigh fading channel," Wireless Personal Communications, vol.2, pp.335–356, 1996.
- [4] S.B. Weinstein and P.M. Ebert, "Data transmission by frequency-division multiplexing using the discrete Fourier transform," IEEE Trans. Commun., vol.COM-19, no.5, pp.628–634, May 1971.
- [5] M. Sawahashi and F. Adachi, "Multicarrier 16QAM transmission with diversity reception," Electron. Lett., vol.32, pp.522–523, March 1996.
- [6] L.J. Cimini, Jr., "Analysis and simulation of a digital mobile channel using orthogonal frequency division multiplexing," IEEE Trans. Commun., vol.COM-33, no.7, pp.665–675, July 1985.
- [7] L. Hanzo, W. Webb, and T. Keller, Single- and multicarrier quadrature amplitude modulation, John Wiley & Sons, 2000.
- [8] M. Helard, R. Le Gouable, J.-F. Helard, and J.-Y. Baudais, "Multicarrier CDMA techniques for future wideband wireless networks," Ann. Telecommun., vol.56, pp.260–274, 2001.
- [9] S. Hara and R. Prasad, "Design and performance of multicarrier CDMA system in frequency-selective Rayleigh fading channels," IEEE Trans. Veh. Technol., vol.48, no.5, pp.1584–1595, Sept. 1999.
- [10] S. Hara and R. Prasad, "Overview of multicarrier CDMA," IEEE Commun. Mag., vol.35, no.12, pp.126–144, Dec. 1997.
- [11] W.C. Jakes, Jr., ed., Microwave mobile communications, Wiley, New York, 1974.
- [12] T. Sao and F. Adachi, "Suppression of noise enhancement for reception of OFDM-CDM signals in a frequency-selective fading channel," 442nd Transmission Eng. Research Colloquium, Tohoku Univ., June 2001.
- [13] H. Atarashi and M. Sawahashi, "Variable spreading factor orthogonal frequency and code division multiplexing (VSF-OFCDM)," 2001 Third International Workshop on Multi-Carrier Spread Spectrum (MC-SS 2001) & Related Topics, pp.113–122, Oberpfafenhofen, Germany, Sept. 2001.
- [14] H. Andoh, M. Sawahashi, and F. Adachi, "Channel estimation filter using time-multiplexed pilot channel for coherent RAKE combining in DS-CDMA mobile radio," IEICE Trans. Commun., vol.E81-B, no.7, pp.1517–1526, July 1998.
- [15] F. Adachi, M. Sawahashi, and H. Suda, "Wideband DS-CDMA for next generation mobile communications systems," IEEE Commun. Mag., vol.36, no.9, pp.56–69, Sept. 1998.
- [16] Proakis, J.G., Digital communications, 2nd ed., McGraw-Hill, 1995.

Appendix

Theoretical BER performance expressions for OFDM-CDMA and DS-CDMA are presented for the single user case ($N = 1$) assuming uniform power delay profile, i.e., $E[|\xi_i|^2] = 1/L$, and ideal channel estimation.

Frequency selective Rayleigh fading channel: When the frequency-domain MRC is applied, the signal-to-noise power ratio per symbol (SNR per symbol) γ is given by

$$\begin{aligned} \gamma &= \frac{\frac{S}{K} \left(\sum_{k=0}^{K-1} |H(k/T_s)|^2 \right)^2}{\sum_{k=0}^{K-1} \frac{N_0}{T_s} |H(k/T_s)|^2} \\ &= 2 \frac{E_b}{N_0} \left(1 - \frac{T_g}{T_s} \right) \left(\frac{1}{K} \sum_{k=0}^{K-1} |H(k/T_s)|^2 \right) \end{aligned}$$

for frequency-domain MRC, (A.1)

where the time dependency of γ is omitted in the equation for simplicity purpose; the signal energy per information bit E_b equals $ST_s/2$ for QPSK data modulation. It is assumed that the channel transfer function remains almost constant over several consecutive sub-carriers, while the minimum delay difference is much larger than T_s/K (FFT sampling period), i.e., $\tau_l - \tau_m \gg T_s/K$. Then, we have

$$\begin{aligned}
& \frac{1}{K} \sum_{k=0}^{K-1} |H(k/T_s)|^2 \\
& \approx \frac{1}{K/T_s} \int_0^{K/T_s} |H(f)|^2 df \\
& = \frac{1}{K/T_s} \int_{-\infty}^{\infty} \int_{-\infty}^{\infty} h(\tau) h^*(\tau') \\
& \quad \cdot \left(\int_0^{K/T_s} \exp[-j2\pi f(\tau - \tau')] df \right) d\tau d\tau' \\
& = \sum_{l=0}^{L-1} \sum_{m=0}^{L-1} \xi_l \xi_m^* F(\tau_l - \tau_m) \quad (\text{A} \cdot 2)
\end{aligned}$$

with

$$F(x) = \exp(j\pi x K/T_s) \frac{\sin(\pi x K/T_s)}{\pi x K/T_s}. \quad (\text{A} \cdot 3)$$

Since $F(x)$ is a rapidly decaying function of x , $F(\tau_l - \tau_m) \approx 0$ if $\tau_l \neq \tau_m$ and Eq. (A·2) becomes

$$\frac{1}{K} \sum_{k=0}^{K-1} |H(k/T_s)|^2 \approx \sum_{l=0}^{L-1} |\xi_l|^2. \quad (\text{A} \cdot 4)$$

Hence,

$$\gamma \approx \frac{2E_b}{N_0} \left(1 - \frac{T_g}{T_s}\right) \sum_{l=0}^{L-1} |\xi_l|^2. \quad (\text{A} \cdot 5)$$

For QPSK modulation, the conditional BER is given by [16]

$$p_b(\gamma) = \frac{1}{2} \operatorname{erfc} \sqrt{\gamma/2}, \quad (\text{A} \cdot 6)$$

where $\operatorname{erfc}(\cdot)$ is the complementary error function. The average BER can be obtained from

$$P_b(E_b/N_0) = \int_0^{\infty} \frac{1}{2} \operatorname{erfc} \sqrt{\gamma/2} p(\gamma) d\gamma, \quad (\text{A} \cdot 7)$$

where $p(\gamma)$ is the probability density function (pdf) of γ . For the uniform power delay profile, $p(\gamma)$ is given by [Eq. (7.4.13), 16]

$$p(\gamma) = \frac{1}{(L-1)!} \frac{\gamma^{L-1}}{\Gamma^L} \exp(-\gamma/\Gamma), \quad (\text{A} \cdot 8)$$

where Γ is the average SNR per symbol given by

$$\Gamma = \frac{2E_b/N_0}{L} \left(1 - \frac{T_g}{T_s}\right). \quad (\text{A} \cdot 9)$$

Finally, the average BER is obtained from [Eq. (7.4.15), 16] as

$$\begin{aligned}
& P_b(E_b/N_0) \\
& = \left(\frac{1-\mu}{2}\right) \sum_{l=0}^{L-1} \binom{L-1+l}{l} \left(\frac{1+\mu}{2}\right)^l, \quad (\text{A} \cdot 10)
\end{aligned}$$

with

$$\mu = \sqrt{\frac{\Gamma/2}{1+\Gamma/2}}. \quad (\text{A} \cdot 11)$$

It is worthwhile noticing that the SNR per symbol of OFDM-CDMA with the frequency-domain MRC is identical to that of DS-CDMA with ideal rake combining, but with $T_g = 0$ in Eq. (A·5). Therefore, the BER expression for OFDM-CDMA is the same as DS-CDMA with $T_g = 0$.

On the other hand, if the ORC frequency equalization is applied, we have

$$\begin{aligned}
\gamma & = \frac{\left(\sum_{k=0}^{K-1} \sqrt{\frac{S}{K}}\right)^2}{\sum_{k=0}^{K-1} \frac{N_0}{T_s} |H(k/T_s)|^{-2}} \\
& = \frac{2\frac{E_b}{N_0} \left(1 - \frac{T_g}{T_s}\right)}{\frac{1}{K} \sum_{k=0}^{K-1} |H(k/T_s)|^{-2}} \quad \text{for ORC}, \quad (\text{A} \cdot 12)
\end{aligned}$$

the pdf of which is quite difficult to derive if not impossible and is not treated here.

Frequency nonselective fading: If only one path ($L = 1$) exists, the channel becomes frequency nonselective and the channel transfer function is $H(f) = \xi_0$ over the entire signal bandwidth. Both Eqs. (A·1) and (A·12) reduce to

$$\gamma = \frac{2E_b}{N_0} \left(1 - \frac{T_g}{T_s}\right) |\xi_0|^2 \quad \text{for MRC and ORC}. \quad (\text{A} \cdot 13)$$

Hence, the theoretical average BER can be obtained simply by letting $L = 1$ in Eq. (A·10).

AWGN channel: The BER performances of OFDM-CDMA and DS-CDMA in the AWGN channel is given by

$$\begin{aligned}
& p_b(E_b/N_0) \\
& = \begin{cases} \frac{1}{2} \operatorname{erfc} \sqrt{\frac{E_b}{N_0} \left(1 - \frac{T_g}{T_s}\right)} \\ \quad \text{for OFDM-CDMA (frequency-domain} \\ \quad \text{MRC and ORC)} \\ \frac{1}{2} \operatorname{erfc} \sqrt{\frac{E_b}{N_0}}, \quad \text{for DS-CDMA} \end{cases} \quad (\text{A} \cdot 14)
\end{aligned}$$



Tomoki Sao received his B.S. degree in communications engineering from Tohoku University, Sendai, Japan, in 2001. Currently, he is a graduate student at the Department of Electrical and Communications Engineering, Tohoku University. His research interests include broadband wireless access using OFDM and CDMA for cellular mobile communications systems. He was a recipient of 2002 IEICE Active Research Award in Radio Commu-

nication Systems.



Fumiyuki Adachi received his B.S. and Dr.Eng. degrees in electrical engineering from Tohoku University, Sendai, Japan, in 1973 and 1984, respectively. In April 1973, he joined the Electrical Communications Laboratories of Nippon Telegraph & Telephone Corporation (now NTT) and conducted various types of research related to digital cellular mobile communications. From July 1992 to December 1999, he was with NTT Mobile

Communications Network, Inc. (now NTT DoCoMo, Inc.), where he led a research group on wideband/broadband CDMA wireless access for IMT-2000 and beyond. Since January 2000, he has been with Tohoku University, Sendai, Japan, where he is a Professor of Electrical and Communication Engineering at Graduate School of Engineering. His research interests are in CDMA and TDMA wireless access techniques, CDMA spreading code design, Rake receiver, transmit/receive antenna diversity, adaptive antenna array, bandwidth-efficient digital modulation, and channel coding, with particular application to broadband wireless communications systems. From October 1984 to September 1985, he was a United Kingdom SERC Visiting Research Fellow in the Department of Electrical Engineering and Electronics at Liverpool University. From April 1997 to March 2000, he was a visiting Professor at Nara Institute of Science and Technology, Japan. He was a co-recipient of the IEICE Transactions best paper of the year award 1996 and again 1998. He is an IEEE Fellow and was a co-recipient of the IEEE Vehicular Technology Transactions best paper of the year award 1980 and again 1990 and also a recipient of Avant Garde award 2000.